Electronic Supplementary Information

Mycelial Pellet-Derived Heteroatom-Doped Carbon Nanosheets with Three-Dimensional Hierarchical Porous Structure for Efficient Capacitive Deionization

Yajing Huang [a#], Jingling Yang [a#], Lingling Hu [a], Dehua Xia [a, b*], Qing Zhang [a], Yuhong Liao [a], Haoyue Li [a], Wenjing Yang [a], Chun He [a, b*], Dong Shu [c]

[a] *School of Environmental Science and Engineering, Sun Yat-sen University, Guangzhou, 510275, China*

[b] *Guangdong Provincial Key Laboratory of Environmental Pollution Control and Remediation Technology, Guangzhou, 510275, China*

[c] *Key Lab of Technology on Electrochemical Energy Storage and Power Generation in Guangdong Universities, School of Chemistry and Environment, South China Normal University, Guangzhou, 510006, China*

(18 Pages including supplementary 3 Tables and 12 Figures)

[#] Yajing Huang and Jingling Yang contributed equally to this work.

[*] Corresponding author: School of Environmental Science and Engineering, Sun Yat-sen University, Guangzhou, 510275, China. Tel.: +86 20 39332690. Email address: xiadehua3@mail.sysu.edu.cn (D.H. Xia); hechun@mail.sysu.edu.cn (C. He).

Table of Contents

NSHPC at different concentrations of NaCl solutions at 1.2 V.

Figure S12. Stability of NSC over three adsorption-desorption cycles in 20 mg L^{-1} NaCl solution.

Table S1. Composition ratio of XPS analysis of MPC and NSHPC.

Sample	Elemental content (at%)			
	C	O	N	S
MPC	91.69	5.05	2.06	0.40
NSHPC	79.77	10.24	4.15	2.94

Table S2. Atomic percentages of various elements N1s and S2p of MPC and NSHPC calculated by the relative areas of corresponding XPS components.

	Element	MPC	NSHPC
N	Pyridinic-N	38.63 %	21.30 %
	Pyrrolic-N	26.38 %	34.07 %
	Graphitic-N	34.98 %	38.03 %
	Oxidized-N	-	6.60 %
S	C-S/C=S S2p	73.13 %	48.11 %
	-C-SO_x	26.87 %	14.74 %
	S^{2-}	-	37.15%

Table S3. Electrochemical parameters of MPC, NSC, NSGC, NSZC and NSHPC carbon electrodes calculated from EIS spectra.

Sample	R_{ct}[b] (Ω)	ESR[a] (Ω)	R_w[c] (Ω)
NSHPC	1.00	0.90	0.98
NSZC	1.27	0.88	0.30
NSGC	1.84	0.96	1.01
NSC	1.81	0.79	5.30
MPC	9.95	1.05	6.20

[a] R_{ct}, the interfacial charge-transfer resistance calculated by the semicircular diameter at high frequency of Nyquist plot.

[b] ESR, intrinsic ohmic resistance calculated from the intersection of the Nyquist plot at the real part at high frequency region.

[c] R_w, the Warburg diffusion resistance calculated by the projected length of the Warburg region on the real axis.

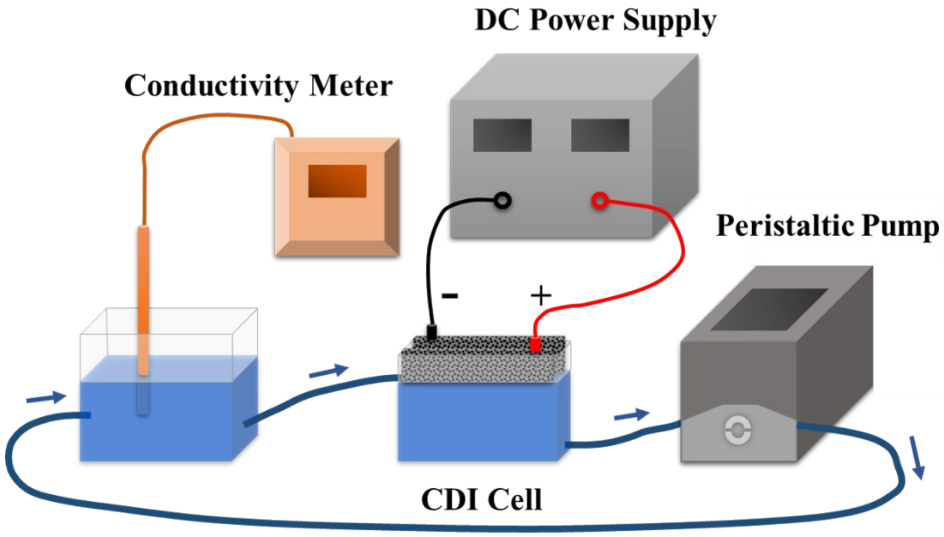

Figure S1. Schematic of capacitive deionization device.

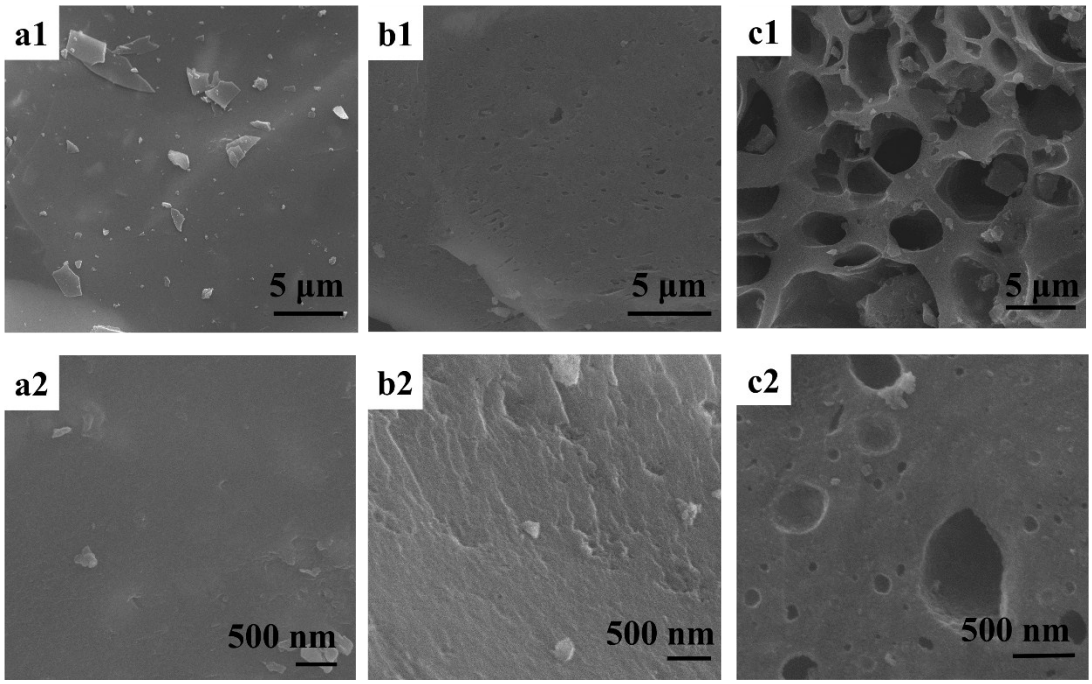

Figure S2. SEM images of NSC (a), NSZC (b) and NSGC (c) samples.

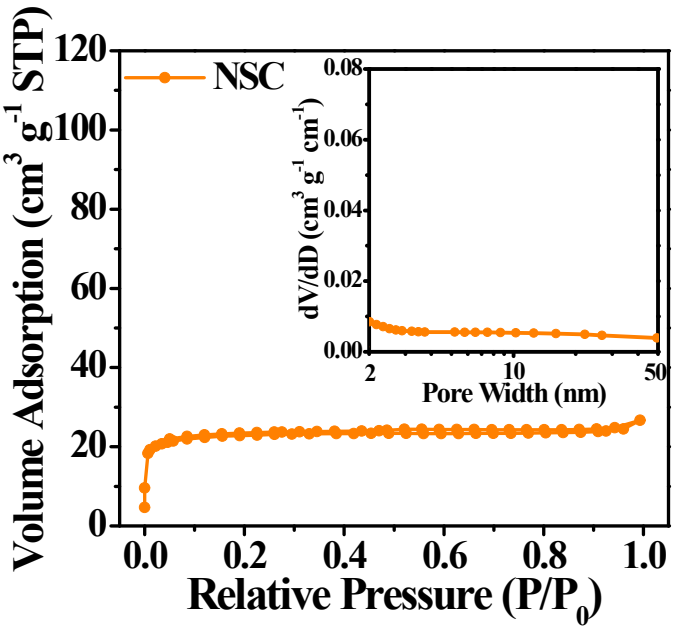

Figure S3. Nitrogen adsorption/desorption isotherms and pore size distributions (inset) of NSC.

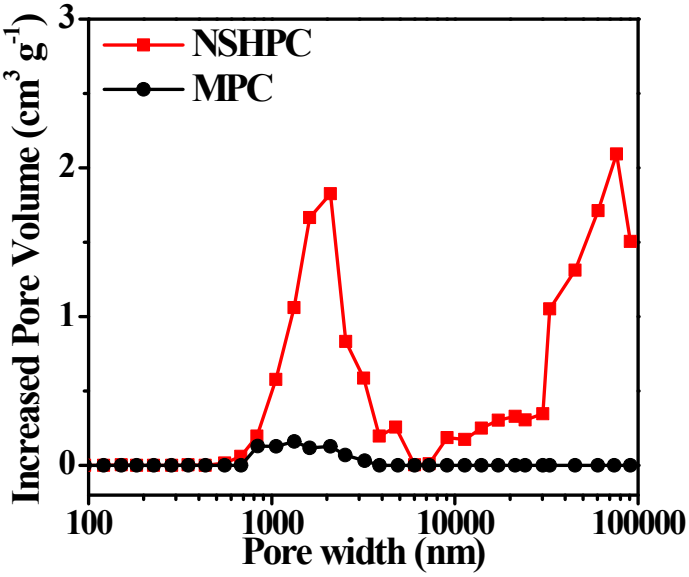

Figure S4. Hg porosimetry analysis of pore volume for MPC and NSHPC.

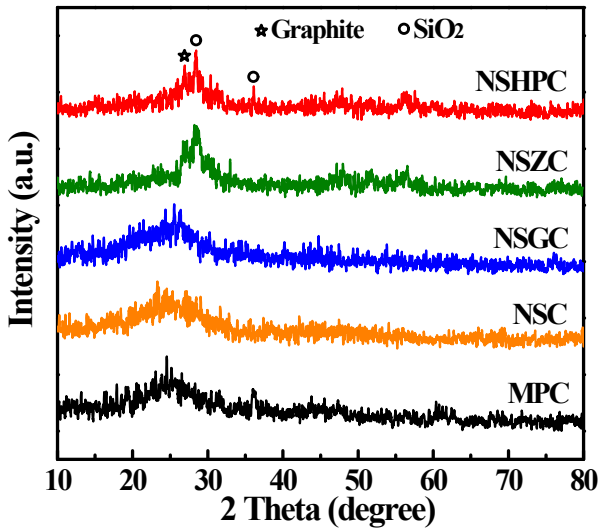

Figure S5. XRD patterns of MPC, NSC, NSGC, NSZC and NSHPC.

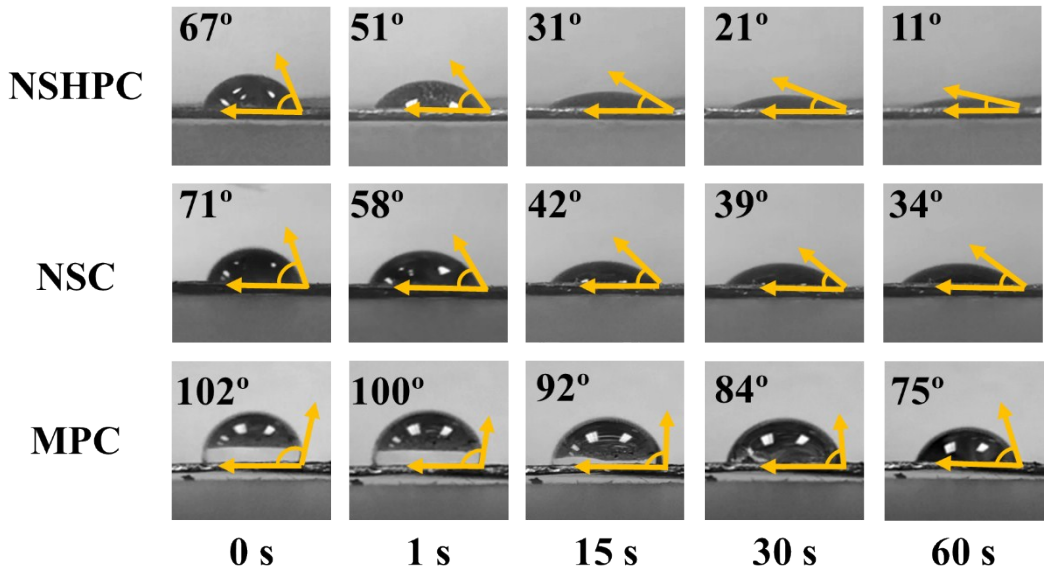

Figure S6. Water contact angle measurements of MPC, NSC and NSHPC electrodes at different contact time.

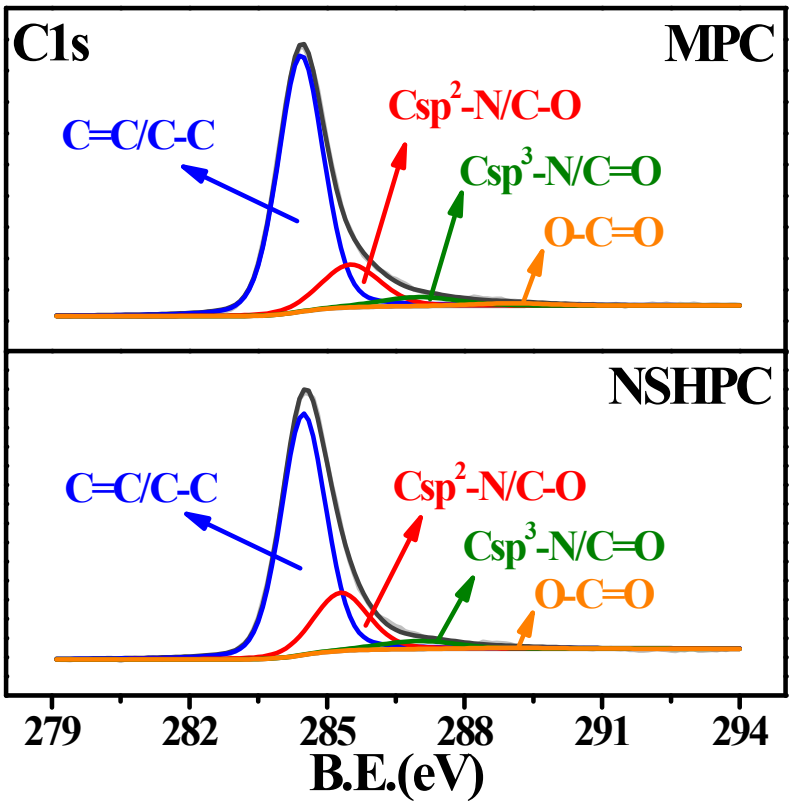

Figure S7. XPS C1s spectra of MPC and NSHPC samples.

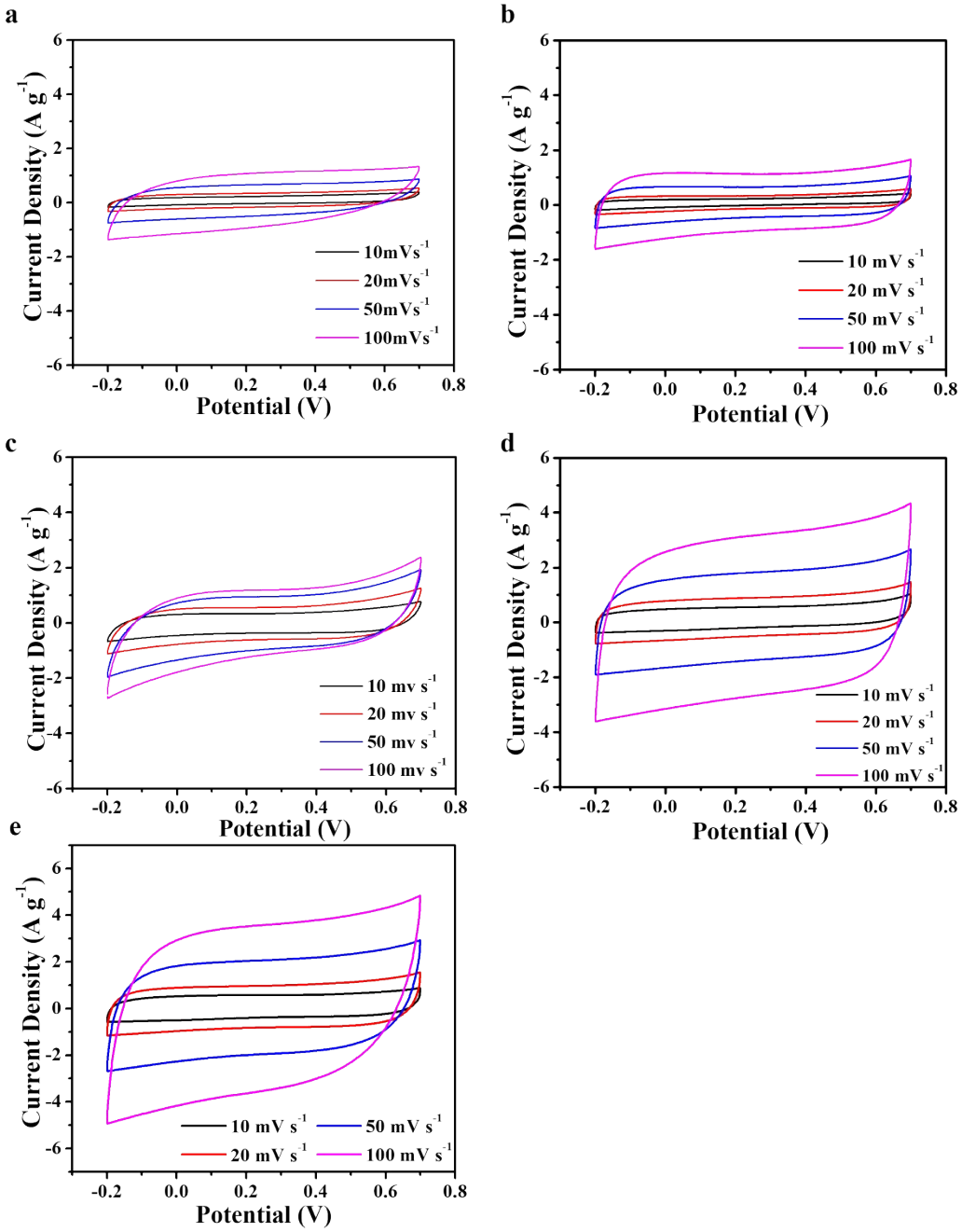

Figure S8. Cyclic voltammetry of MPC (a), NSC (b), NSGC (c), NSZC (d), and NSHPC (e) at different scan rates in 1.0 M NaCl aqueous solution.

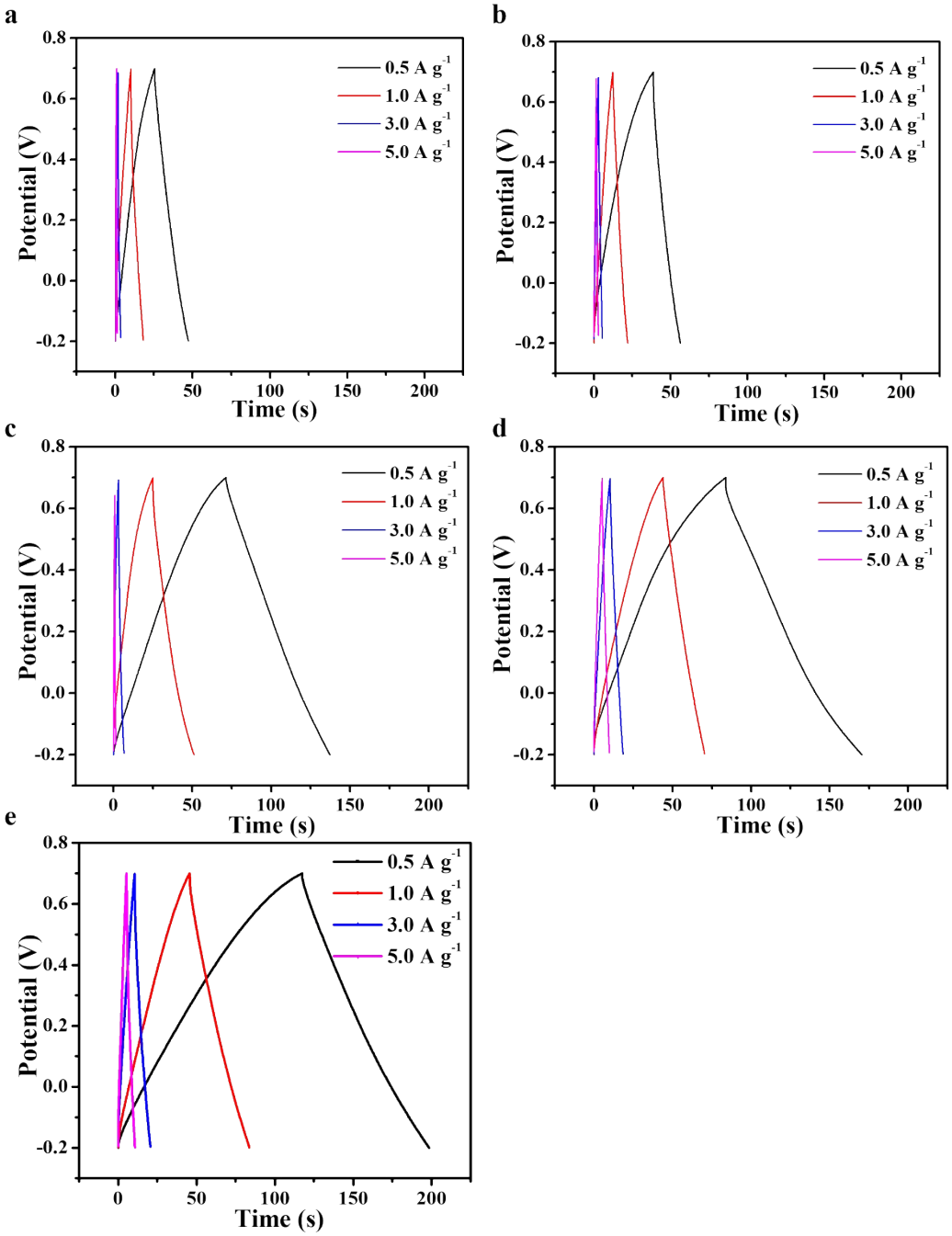

Figure S9. Galvanostatic charge-discharge curves of MPC (a), NSC (b), NSGC (c), NSZC (d), and NSHPC (e) at different current density in 1.0 M NaCl aqueous solution.

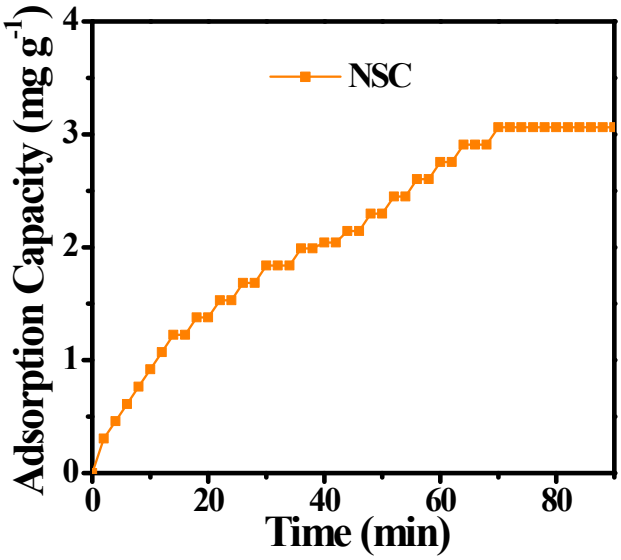

Figure S10. Desalination performance of NSC in 20 mg L^{-1} NaCl solution.

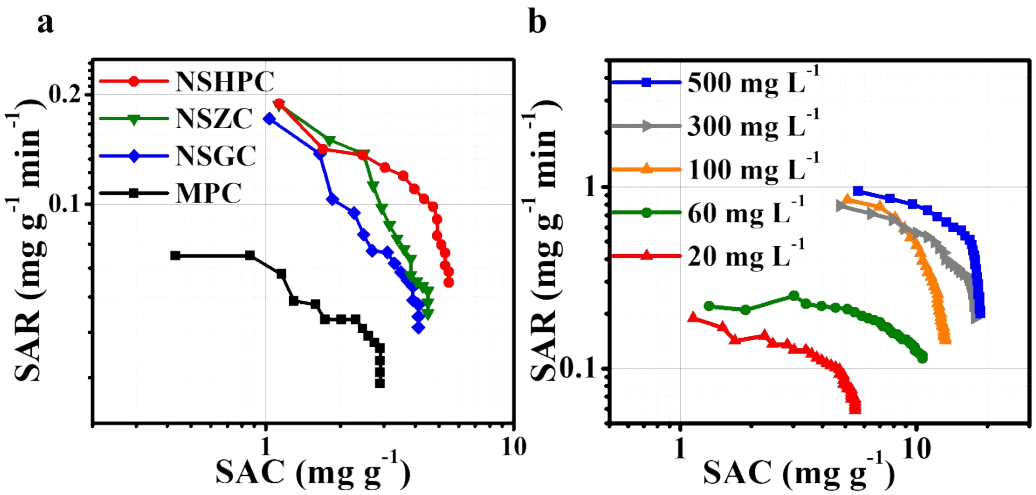

Figure S11. (a) Ragone plots of SAC *vs.* SAR for MPC, NSGC, NSZC and NSHPC electrodes in a 20 mg L^{-1} NaCl solution at 1.2 V. (b) Ragone plots of SAC *vs.* SAR of NSHPC at different concentrations of NaCl solutions at 1.2 V.

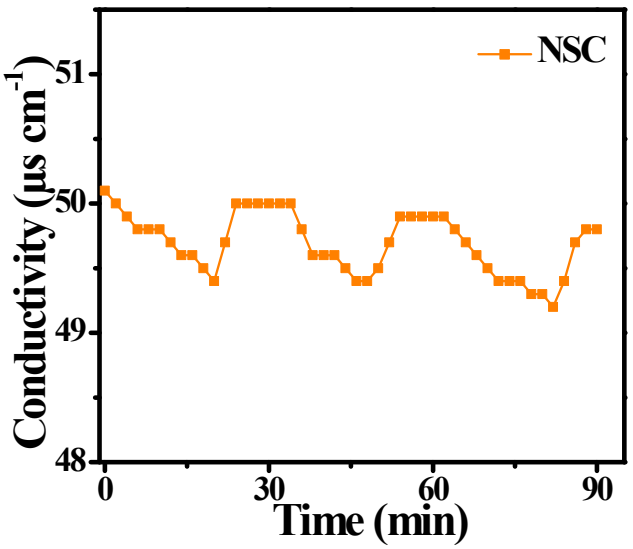

Figure S12. Stability of NSC over three adsorption-desorption cycles in 20 mg L^{-1} NaCl solution.